BJCP British Journal of Clinical Pharmacology

DOI:10.1111/j.1365-2125.2011.04015.x

A mechanism-based model for the population pharmacokinetics of free and bound aflibercept in healthy subjects

Hoai-Thu Thai,[1,2] Christine Veyrat-Follet,[1] Nicole Vivier,[1] Catherine Dubruc,[1] Gerard Sanderink,[1] France Mentré[2] & Emmanuelle Comets[2]

[1]Global Metabolism and Pharmacokinetics Department, Sanofi-aventis and [2]UMR738, INSERM, University Paris Diderot, Paris, France

Correspondence
Ms Hoai-Thu Thai, UMR738, INSERM, University Paris Diderot, 16 rue Henri-Huchard, 75018 Paris, France.
Tel.: +33 1 5727 7538
Fax: +33 1 5727 7521
E-mail: hoai-thu.thai@inserm.fr

Keywords
aflibercept, MONOLIX, population pharmacokinetics, target-mediated drug disposition, VEGF

Received
1 December 2010

Accepted
7 May 2011

Accepted Article
17 May 2011

WHAT IS ALREADY KNOWN ABOUT THIS SUBJECT

- Anti-angiogenic drugs have been developed as an effective therapeutic strategy for inhibiting tumour growth. However, their pharmacokinetics (PK) and their ligand inhibition properties have not been well characterized. The binding to a circulating target, such as vascular endothelial growth factor (VEGF), makes the PK of these drugs more complex.

WHAT THIS STUDY ADDS

- The underlying mechanism of disposition of aflibercept, where a saturable and high affinity binding of aflibercept to VEGF was adequately characterized by the Michaelis–Menten approximation of a target-mediated drug distribution model. To our knowledge, this is the first published mechanism-based population PK model for an anti-VEGF drug.

AIM

Aflibercept (VEGF-Trap), a novel anti-angiogenic agent that binds to VEGF, has been investigated for the treatment of cancer. The aim of this study was to develop a mechanism-based pharmacokinetic (PK) model for aflibercept to characterize its binding to VEGF and its PK properties in healthy subjects.

METHODS

Data from two phase I clinical studies with aflibercept administered as a single intravenous infusion were included in the analysis. Free and bound aflibercept concentration–time data were analysed using a nonlinear mixed-effects modelling approach with MONOLIX 3.1.

RESULTS

The best structural model involved two compartments for free aflibercept and one for bound aflibercept, with a Michaelis–Menten type binding of free aflibercept to VEGF from the peripheral compartment. The typical estimated clearances for free and bound aflibercept were 0.88 l day^{-1} and 0.14 l day^{-1}, respectively. The central volume of distribution of free aflibercept was 4.94 l. The maximum binding capacity was 0.99 mg day^{-1} and the concentration of aflibercept corresponding to half of maximum binding capacity was 2.91 µg ml^{-1}. Interindividual variability of model parameters was moderate, ranging from 13.6% (V_{max}) to 49.8% (Q).

CONCLUSION

The present PK model for aflibercept adequately characterizes the underlying mechanism of disposition of aflibercept and its nonlinear binding to VEGF.

Introduction

Angiogenesis, the development of new blood vessels from pre-existing vasculature, participates in a variety of physiological processes and disease states [1]. Its critical role in tumour development and progression was established 30 years ago [2]. This discovery brought a new effective approach called anti-angiogenic therapy to cancer treatment, which consists in limiting blood supply to tumours by preventing angiogenesis. The development of new agents has attracted many researchers' interest in the pharmaceutical industry. To date, the best characterized and most highly validated anti-angiogenic approach involves targeting the vascular endothelial growth factor (VEGF) pathway [3].

Vascular endothelial growth factor is the most potent pro-angiogenic growth factor, promoting the formation of blood vessels which are required for both normal and neoplastic tissue growth [1, 4]. VEGF binds to two high-affinity receptors (VEGFR-1 and VEGFR-2) on endothelial cells. This binding activates the intrinsic tyrosine kinase activity of their cytodomains, initiating intracellular signalling. VEGF is expressed in a large variety of malignant tumours, such as tumours of the breast, brain, lung and gastrointestinal tract [5]. Blockade of the VEGF pathway is therefore an effective therapeutic strategy for inhibiting tumour growth [4–6].

Aflibercept (also called VEGF-Trap, Regeneron Pharmaceutics/Sanofi-aventis research) is a novel anti-angiogenic agent that binds to VEGF with a 1:1 ratio and prevents it from interacting with its receptors. A recombinant fusion protein consisting of the second Ig domain of VEGFR-1 and the third Ig domain of VEGFR-2 fused to the Fc portion of human immunoglobin IgG1, it has a higher affinity for VEGF-A (K_d *in vitro* = 0.5 pM) than current anti-VEGF monoclonal antibodies [7–9]. Aflibercept also binds to VEGF-B and Placental Growth Factor (PlGF), which may be advantageous in some settings, such as malignant ascites where PlGF may mediate vascular permeability [9].

Based on the mechanism of action, this drug undergoes a target-mediated drug disposition (TMDD), a term used to describe the phenomenon in which drug is bound with high affinity to its pharmacologic target such that this interaction is reflected in the pharmacokinetic properties of the drug. A general PK model for drugs exhibiting TMDD has been developed by Mager *et al*. [10, 11]. This model describes the elimination pathway of drug plasma concentrations as the combination of first-order elimination from the central compartment and specific target binding clearance followed by internalization of the drug–target complex. It also characterizes the turnover of the target. The full TMDD model is complex and generally overparameterized. The more information we have about free drug, bound drug and the target, the more TMDD model components and parameters can be adequately identified, although it is yet unclear which elements should be measured to estimate all the parameters in the full TMDD model. In order to overcome this problem, several simpler forms of the TMDD model were proposed [12, 13]. There are mainly three approximations: quasi equilibrium (QE), quasi steady-state (QSS) and Michaelis–Menten (MM). The QE approximation is based on the assumption that the drug–target binding is much faster than all other system processes. If the rate of elimination of the complex is not negligible, the QE approximation is replaced by the QSS approximation assuming that the drug–target complex concentration changes more slowly than the binding and internalization process. The MM approximation describes the system when the target concentration is small relative to the free drug concentration and the dosing regimens result in the target being fully saturated [13].

Pharmacokinetics (PK) of aflibercept were investigated in healthy subjects after single intravenous (i.v.) doses of 1 to 4 mg kg^{-1} and a single subcutaneous (s.c.) dose of 2 mg kg^{-1}, in two phase 1 clinical studies as part of the drug's clinical development. Both free and bound aflibercept concentrations were assayed. The objective of this analysis was to develop a mechanism-based PK model for aflibercept in order to characterize its binding to VEGF and its pharmacokinetic properties in healthy subjects. The influence of covariate was not assessed in this study due to the limited number of individuals and their healthy status.

Methods

Study design

The data for the population PK analysis were collected from two phase 1, monocentric and randomized studies which were both carried out in healthy male subjects to assess the PK of aflibercept. The studies were approved by the independent ethics committees (Pharma-Ethics, South Africa and Ethik-Kommission der Landesärztekammer Baden-Württemberg, Germany). They were performed according to recommendations of the 18th World Health Congress (Helsinki, 1964) and all applicable amendments. The volunteers gave their written informed consent after full explanation of all procedures involved in the studies.

Study 1 was a placebo-controlled, single-dose, sequential ascending-dose study. Forty-eight subjects were enrolled in this study and equally divided into four groups: one group receiving placebo and three groups receiving a single dose of 1, 2 or 4 mg kg^{-1} of aflibercept, respectively, administered as a 1-h i.v. infusion.

Study 2 was an open-label, single-dose, crossover study. Two groups of 20 subjects were included in the study. The first group received a single i.v. dose of 2 mg kg^{-1} in the first period, with a 2-month follow-up period, followed by a single s.c. dose of 2 mg kg^{-1} in the second period. The second group received the s.c. dose first, then the i.v. dose.

The data from s.c. administration in the crossover study (study 2) were removed from the analysis because this route of administration was not pursued in the subsequent

clinical development. Moreover, in this study, a carry-over effect was found and should have been taken into account in the modelling, but this required the modelling of the s.c. route. To avoid it and to work on homogenous data, only the i.v. infusion data in the first period were used in the population analysis.

Blood sampling schedules

In study 1, blood samples (4 ml) were taken at the following times: pre dose, 1 (end of infusion), 2, 4, 6, 8, 12 and 24 h post start of administration on day 1, then on days 8, 15, 22, 29, 36 and 43 at the same morning time corresponding to 2 h after the start of infusion on day 1.

In study 2, blood samples (4 ml) were taken at the following times: pre dose, 1, 2, 4, 6 and 8 h post start of administration on day 1, then on days 2, 3, 5, 8, 15, 2 and 43 of each period at the same morning time corresponding to 2 h after the start of infusion on day 1.

Assay method

For both studies, free and bound aflibercept plasma concentrations were measured in all samples collected at Regeneron Pharmaceuticals, Inc. using enzyme-linked immunosorbent assay (Elisa) method. Blood samples were collected in tubes (containing 1 ml of citrate buffer, sodium citrate, and 4.2 mg of citric acid) and were centrifuged at 2000 *g* for 15 min at room temperature. Plasma was stored at −20°C until analysed.

In the assay of free aflibercept, human VEGF165 was initially adsorbed to the surface of a polystyrene solid support to capture the free aflibercept in the samples. A mouse monoclonal antibody (reporter antibody), specific to an epitope on the VEGFR1 domain of aflibercept, was then bound to the immobilized complex and an enzyme-linked antibody (peroxidase-conjugated Affinipure goat anti-mouse IgG Fc-γ) was bound to the immobilized mouse monoclonal complex. A luminal-based substrate specific for peroxidase was added to achieve a signal intensity that was directly proportional to the concentration of free aflibercept. The limit of quantification of free aflibercept was 15.6 ng ml^{-1}. The calibration curves ranged from 100 ng ml^{-1} to 1.56 ng ml^{-1} in twofold serial dilution. The limit of quantification of free aflibercept was 15.6 ng ml^{-1}. The inter-day accuracy and precision ranged from 92.24% to 103.09% and 1.05% to 16.18%, respectively. The intra-day accuracy and precision ranged from 106.36% to 109.90% and 9.56% to 13.68%, respectively.

In the assay of bound aflibercept, human VEGF165 was replaced by a non-blocking goat anti-human VEGF antibody for capturing the bound aflibercept in subject samples. The rest of the procedure was similar to the one used in the assay of free aflibercept. The limit of quantification for bound aflibercept was 43.9 ng ml^{-1}. The calibration curves ranged from 100 ng ml^{-1} to 8.78 ng ml^{-1} in a 1.5 serial dilution. The inter-day accuracy and precision ranged from 93.85% to 110.19% and 0.38% to 16.17%, respectively. The intra-day accuracy and precision ranged from 115.70% to 123.34% and 1.09% to 1.58%, respectively.

Population PK analysis

The population PK analysis was performed using the MONOLIX program (version 3.1) implementing the SAEM algorithm. The model control files were written using MLXTRAN script. The early concentrations of bound aflibercept were often below the limit of quantification, thus the censored data of bound aflibercept, representing 32.5% of data, were taken into account and used for model development using the extended SAEM algorithm implemented in MONOLIX as an exact maximum likelihood estimation method [14]. In this algorithm, the left-censored data are simulated in a right-truncated Gaussian distribution, instead of being imputed by the LOQ value or half of the LOQ value. The data of bound aflibercept contains also some observed concentrations which were reported with values below the LOQ reported for most of the data (see bottom left plot in Figure 4).

The database included a total of 56 subjects, with 36 subjects receiving treatments from study 1 and 20 subjects receiving i.v. infusions in the first period from study 2. With respect to the law of mass action, the concentrations of bound aflibercept were converted into equivalent concentrations of free aflibercept by multiplying them with 0.717, the ratio of molecular weights between free and bound aflibercept. The units of free aflibercept and bound aflibercept concentrations were μg ml^{-1} and μg eq ml^{-1} respectively.

Pharmacokinetic structural model

The following strategy was used to develop the model. Free aflibercept concentration–time data were first modelled alone. Then, bound concentration–time data were included for simultaneous modelling.

The structural model for free aflibercept was developed by testing the following models: two-compartment or three-compartment models with first-order and/or MM elimination.

In the next step, we developed a structural model including bound aflibercept. The TMDD model with association and dissociation rate constants (k_{on} and k_{off}), reduced approximate TMDD models and other simpler models with linear binding constants were used to describe the joint evolution of the two entities.

Statistical model

Denoting *f* the function describing the model, the statistical model for observed concentration C_{ij} of subjects i for sampling time t_{ij} is:

$$C_{ij} = f(\theta_i, t_{ij}) + \varepsilon_{ij}$$

where θ_i is the vector of parameters of subject i and ε_{ij} is the residual error.

The errors ε_{ij} were assumed to be independent and normally distributed with a null mean and a heteroscedastic variance σ^2_{ij}, which was modelled using a combined additive and proportional model:

$$\sigma^2_{ij} = (\sigma_a + \sigma_p f(\theta_i, t_{ij}))^2$$

where σ_a and σ_p are additive and proportional coefficients of the residual error model respectively.

Two alternative residual error models, proportional model ($\sigma_a = 0$) and additive model ($\sigma_p = 0$) were also evaluated for the residual variability.

The interindividual variability on all parameters was modelled with an exponential model, e.g. for CL:

$$CL_i = CL \cdot \exp(\eta_{i,CL})$$

where $\eta_{i,CL}$ denotes the random effect in subject i, CL_i the individual clearance parameter and CL the typical value of the population. The use of an exponential model implies a log-normal distribution for the parameters. The ηs (e.g. $\eta_{i,CL}$) are zero mean random variables with variance ω^2 (e.g. for CL, ω^2CL). The ω^2s represent the variance of the random effects. The elements of the interindividual variance-covariance matrix, Ω, was modelled as diagonal, e.g. assuming no covariance between the ηs.

The following strategy was used for model development. First, the structural PK models were developed with a combined residual error model and interindividual variability on all parameters. Then, the residual error models were evaluated for the selected structural model. Finally, the interindividual variability on each parameter was tested for significance, and the non-significant variability components were removed one by one starting with the smallest and least significant estimate.

The log likelihood (LL) was computed using importance sampling. The likelihood ratio test was used to discriminate between nested models through the difference in log likelihood (–2 LL). A *P*-value of 0.05 was considered statistically significant. For non-nested models, the model selection was based on the Bayesian information criterion (BIC). The better model is the one with a smaller value of BIC [15].

Model evaluation

Internal evaluation of the model was based on goodness-of-fit (GOF) plots, including plots of observations *vs.* individual and population predictions and plots of normalized prediction distribution error (NPDE) [16]. A visual predictive check (VPC) was used to assess model predictive performance, based on the simulation of 500 data sets.

Results

Data

The database for population PK analysis contained data from 56 healthy subjects involved in the two phase 1 clinical studies. A total of 1476 concentrations were used for model building: 732 concentrations of free aflibercept and 744 concentrations of bound aflibercept of which 242 (32.5%) were below the quantification limit (LOQ = 43.9 ng ml^{-1} or 0.0314 μg eq ml^{-1}).

The pooled concentrations of free aflibercept and bound aflibercept plotted *vs.* time are presented in Figure 1.

The time course of free aflibercept after i.v. infusion of doses of 1, 2 and 4 mg kg^{-1} in semi-log scale suggests a bi-exponential decline with a rapid phase of distribution followed by a prolonged terminal phase of elimination regardless of the dose. The time course of bound aflibercept suggests a saturable binding phenomenon with the same observed plateau for the two higher doses. The peaks of complex occurred sooner for 1 mg kg^{-1} and later for doses of 2 and 4 mg kg^{-1} (around 21 days for both doses).

Free aflibercept modelling

Several models were proposed to characterize the kinetics of free aflibercept. In the two-compartment model with first-order elimination, the distribution of *post hoc* clearance for three doses showed a dose-dependent clearance, confirming the nonlinear disposition already observed during non-compartmental analysis. The two-compartment model with MM elimination was then developed and showed a better description of data with a decrease of 33.61 points in –2 LL value. The three-compartment models with first-order or MM elimination were also evaluated. They provided a slight decrease in –2 LL compared with the two-compartment models but the fitting did not show a significant improvement. The two-compartment model with MM elimination was therefore selected as an adequate structural model for free aflibercept.

The best residual error for this model was the combined additive and proportional error. The interindividual variability on K_m was not significant.

Free and bound aflibercept modelling

The binding of aflibercept to VEGF and the nonlinear kinetics of free aflibercept suggests that this drug has target-mediated drug disposition properties. Therefore, the TMDD model with association and dissociation rate constants (k_{on} and k_{off}) reduced approximate TMDD models and other simpler models with linear binding constants were tested. The MM approximation of the TMDD model developed by Gibiansky and colleagues [13] was found to be the best approach to describe the kinetics of both free and bound aflibercept, while others did not fit the concentrations of bound correctly and/or had overparameterization issues. In all of these models, the dissociation rate k_{off} was very small compared with other constants and very badly estimated.

The nonlinear central and peripheral binding of this MM approximate TMDD model were tested and compared.

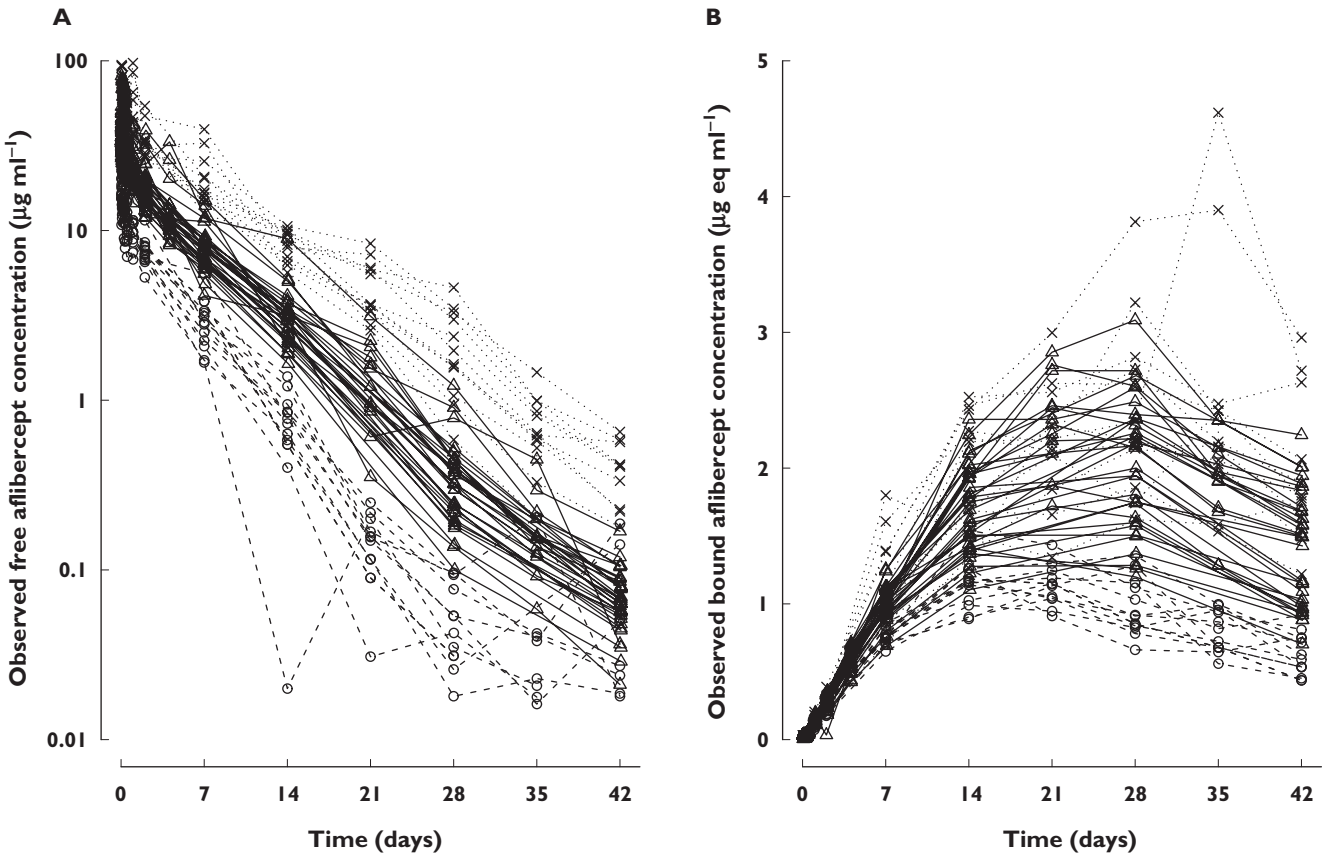

Figure 1

Observed concentrations of (A) free aflibercept (μg ml^{-1}) and (B) bound aflibercept (μg eq ml^{-1}) *vs.* time

The nonlinear peripheral binding model was found to describe the data better than the central binding one with a smaller value of BIC (2160 *vs.* 2703) and therefore was retained as the structural model for free and bound aflibercept.

The final structural model relating free and bound aflibercept is shown in Figure 2.

Free aflibercept in plasma distributes first to tissues then binds to VEGF to form the complex. Binding to VEGF follows the law of mass action and can be characterized by a nonlinear form with MM constants (V_{max} and K_m). The bound aflibercept (complex) is assumed to be directly eliminated through internalization (k_{int}) and not through the dissociation rate constant (k_{off}) which gives back free aflibercept and free VEGF. The concentration of free aflibercept in central compartment (C_p), in the tissue compartment (C_t) and the concentration of bound aflibercept (C_b) are described by means of differential equations:

$$\frac{dC_p}{dt} = \text{Input} - (k_{el} + k_{pt}) \cdot C_p + k_{tp} \cdot \frac{C_t \cdot V_t}{V_p} \quad (1)$$

$$\frac{dC_t}{dt} = k_{pt} \cdot \frac{C_p \cdot V_p}{V_t} - k_{tp} \cdot C_t - \frac{1}{V_t} \cdot \frac{V_{max} \cdot C_t}{K_m + C_t} \quad (2)$$

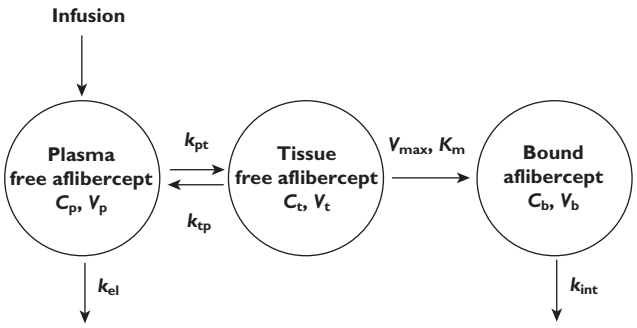

Figure 2

Proposed structural models for free and bound aflibercept (two compartments for free aflibercept, one compartment for bound aflibercept) with binding to VEGF occurring in the peripheral compartment

$$\frac{dC_b}{dt} = \frac{1}{V_b} \cdot \frac{V_{max} \cdot C_t}{K_m + C_t} - k_{int} \cdot C_b \quad (3)$$

in which k_{el} is the first-order elimination rate constant of free aflibercept (day^{-1}) from the central compartment, k_{tp} and k_{pt} are the first-order rate constants between central

and peripheral compartment (day^{-1}), k_{int} is the first-order rate constant of bound aflibercept internalization (day^{-1}), V_{max} is the maximum binding capacity (mg day^{-1}), K_m is the concentration of free aflibercept corresponding to half of maximum binding capacity (μg ml^{-1}), V_p is the central volume of distribution of free aflibercept (l), V_t is the peripheral volume of distribution of free aflibercept and V_b is the volume of distribution of bound aflibercept (l). More details concerning the derivation of the model equations and its relationship to other TMDD models proposed in the literature can be found in the Appendix.

In this model, the volume of bound aflibercept (V_b) and the maximum binding capacity (V_{max}) were however highly correlated with a correlation coefficient higher than 0.95, suggesting identifiability issues. In order to prevent this problem, the value of V_b was assumed to be equal to the value of central volume of distribution of free aflibercept (V_p), corresponding to the hypothesis that free and bound aflibercept are distributed within the same space in the plasma compartment. To do so, V_b was fixed to the population value of V_p with no interindividual variability, instead of being estimated.

The best residual error model of bound aflibercept was the proportional model, while that of free aflibercept was the combined additive and proportional error model found in the first step. A combined error model was also attempted. However, the contribution of the additive error was negligible and was therefore discarded. The interindividual variability on the internalization rate constant (k_{int}) was found to be small (11.9%) and badly estimated. The likelihood ratio test demonstrated that removing this variability from the model did not significantly change the fit.

The estimated parameter values for the best model of free and bound aflibercept are presented in Table 1.

All model parameters were well estimated with relative standard errors (RSE) <20%. The population estimate of clearance for free aflibercept was 0.88 l day^{-1} and the internalization rate for bound aflibercept was 0.028 day^{-1}, resulting in a clearance of 0.14 l day^{-1}. V_p for free aflibercept was 4.94 l. The maximum binding capacity was 0.99 mg day^{-1} and the estimated concentration of free aflibercept corresponding to half of maximum binding capacity was low (2.91 μg ml^{-1}).

Interindividual variability for random effects associated with model parameters was moderate, ranging from 13.6% (V_{max}) to 49.8% (Q). Residual errors were low for both free and bound aflibercept with proportional parts of 17.1% and 12.6% respectively. The additive error of free aflibercept was also small compared with the observed concentrations.

The goodness-of-fit plots of the best joint model are shown in Figure 3. The plots of observations *vs.* population predictions and observations *vs.* individual predictions indicated that the model adequately described the observations over the dose range. The normalized prediction distribution error plots, NPDE *vs.* time and NPDE *vs.* predictions, showed a symmetric distribution around zero, except for the early times and the small concentrations of bound aflibercept. This bias was caused by omitting the NPDE corresponding to below the quantification limit (BQL) observations. For BQL data, the metric NPDE has not yet been developed.

The total number of BQL concentrations of bound aflibercept predicted by the model was 251 (33.73%), 231 of which corresponded to observed BQL data. This shows the good agreement between model prediction and observation for BQL data.

Examples of individual fits taken from two studies with three doses are shown in Figure 4. The model described the observed concentrations of free and bound aflibercept for all subjects quite well.

Figure 5 presents the visual predictive checks for both free and bound aflibercept. The 80% prediction interval and median were obtained by simulating 500 data sets under the final model. In addition, we obtained the 90% prediction intervals around the median and the upper and lower boundaries of the interval. Concentrations lower than the LOQ simulated for free aflibercept at the end of treatment were replaced by the LOQ (0.0156 μg ml^{-1}) in order to obtain a lower limit for the VPC plots on a

Table 1

1-Parameter estimates for the best free and bound model

Fixed effects Parameter	Estimate (RSE%)	Interindividual variability ω (%) (RSE%)	Residual variability	σ_a (μg ml^{-1}) (RSE%)	σ_p(%) (RSE%)
CL (l day^{-1})	0.88 (4.0)	28.0 (10)	Free aflibercerpt	0.05 (9.0)	17.1(3.0)
V_p (l)	4.94 (4.0)	27.3 (10)	Bound aflibercept	–	12.6 (4.0)
Q (l day^{-1})	1.39 (9.0)	49.8 (14)			
V_t (l)	2.33 (7.0)	39.8 (14)			
V_b (l)	4.94 (=V_p)	–			
V_{max} (mg day^{-1})	0.99 (5.0)	13.6 (17)			
K_m (μg ml^{-1})	2.91 (11)	45.6 (15			
k_{int} (day^{-1})	0.028 (5.0)	–			

CL: clearance of free aflibercept from central compartment (CL = k_{el}·Vp). Q: intercompartment clearance of free aflibercept (Q = k_{tp}·V_t = k_{pt}·V_p).

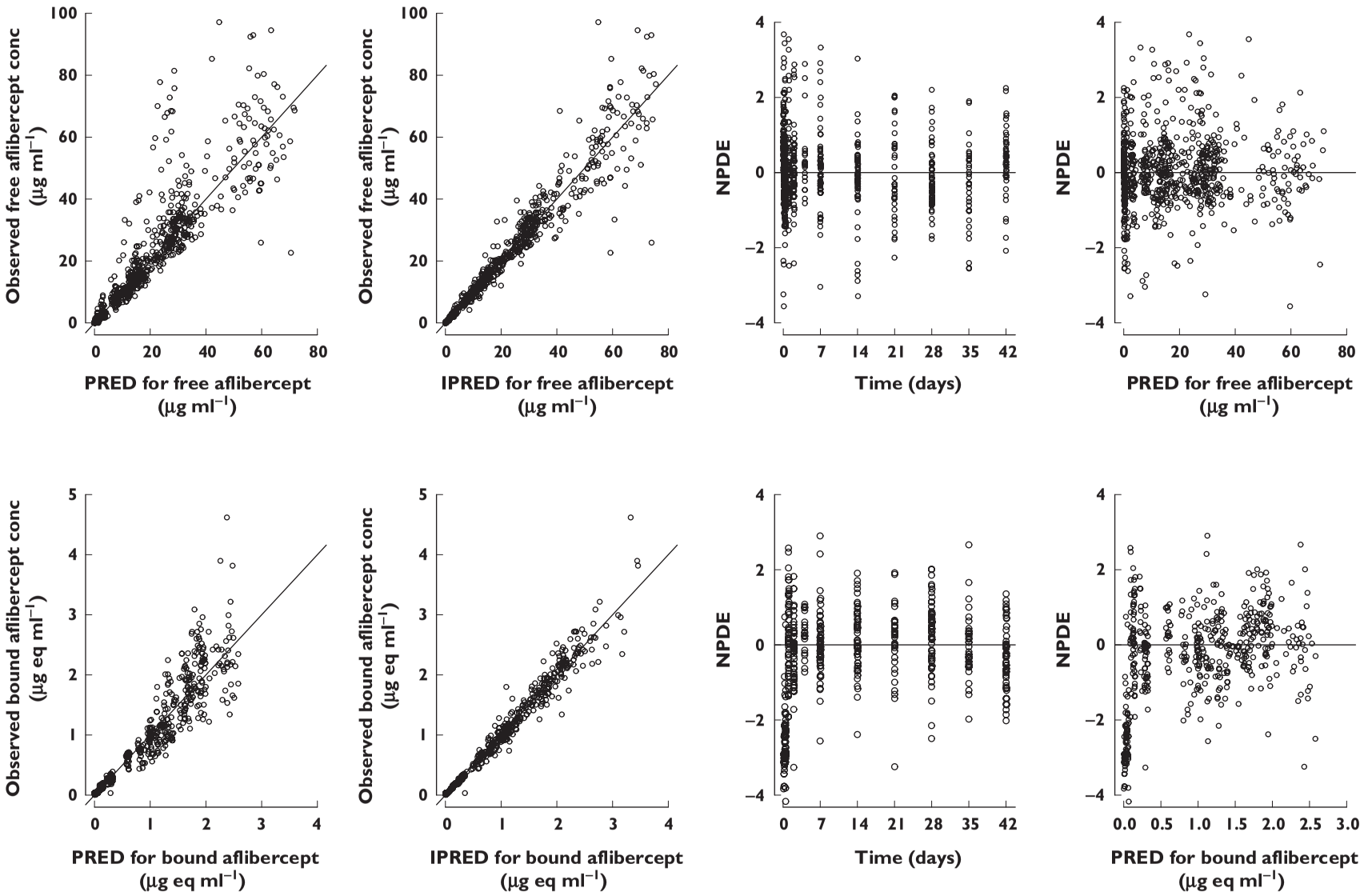

Figure 3

Diagnostic goodness-of-fit plots for the model of free and bound aflibercept, showing observed *vs.* population predicted concentrations (PRED), observed *vs.* individual predicted concentrations (IPRED) and normalized prediction distribution error (NPDE) *vs.* population predicted concentrations. The lower limit of quantification for bound aflibercept was 43.9 ng ml^{-1} (0.0314 μg eq ml^{-1}). BQL observations were removed from the plots

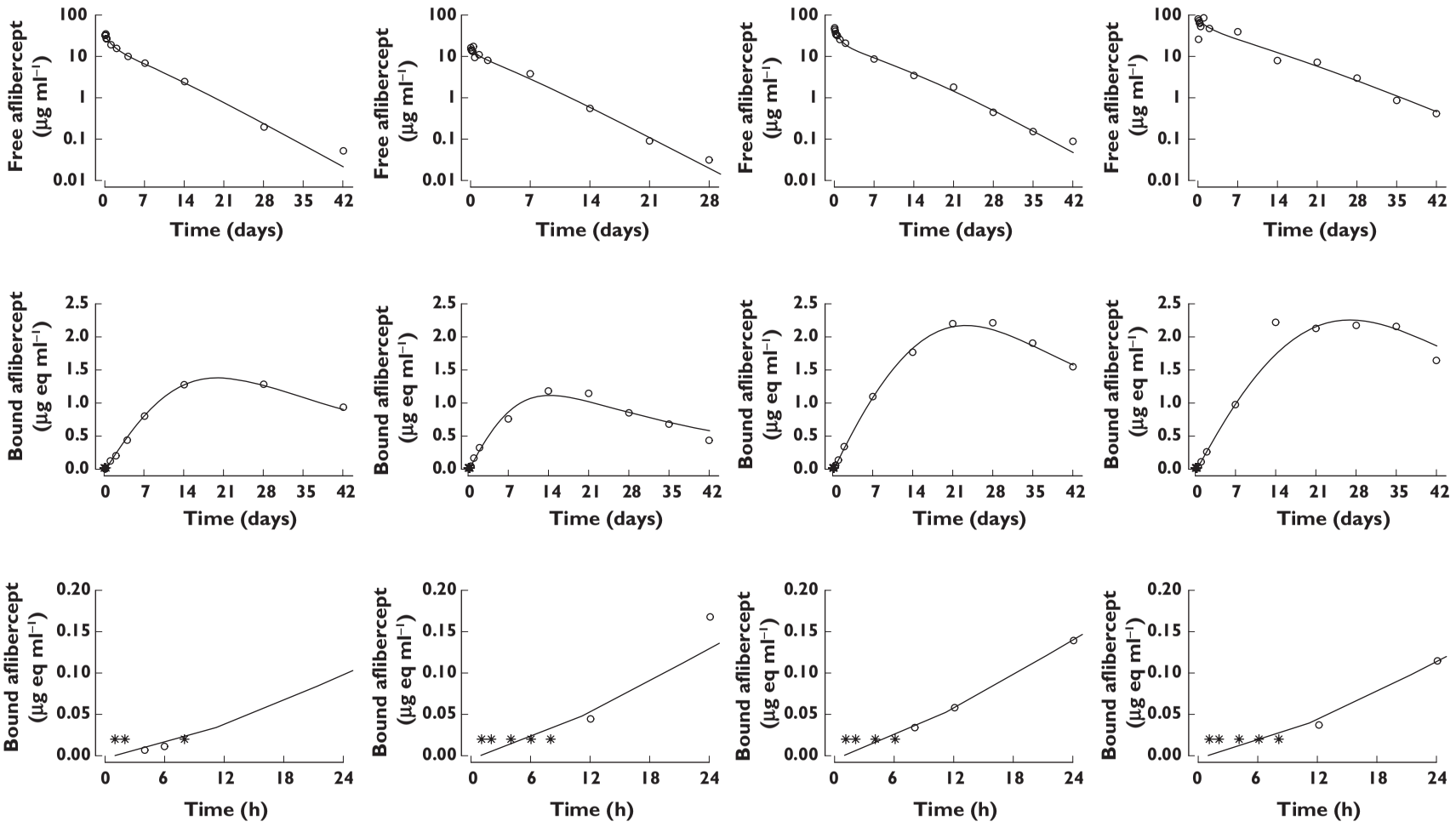

Figure 4

Examples of individual fits for four representative individuals. From left to right: study 1 with dose of 2 mg kg^{-1}, study 2 with dose of 1, 2, 4 mg kg^{-1}. Fits for free aflibercept are presented in the top, bound afibercept in the middle, and the first 24 h fits of bound aflibercept at the bottom. Observed data are plotted using a circle (○) and BQL data are plotted using a star (*). The line (–) represents the prediction of model

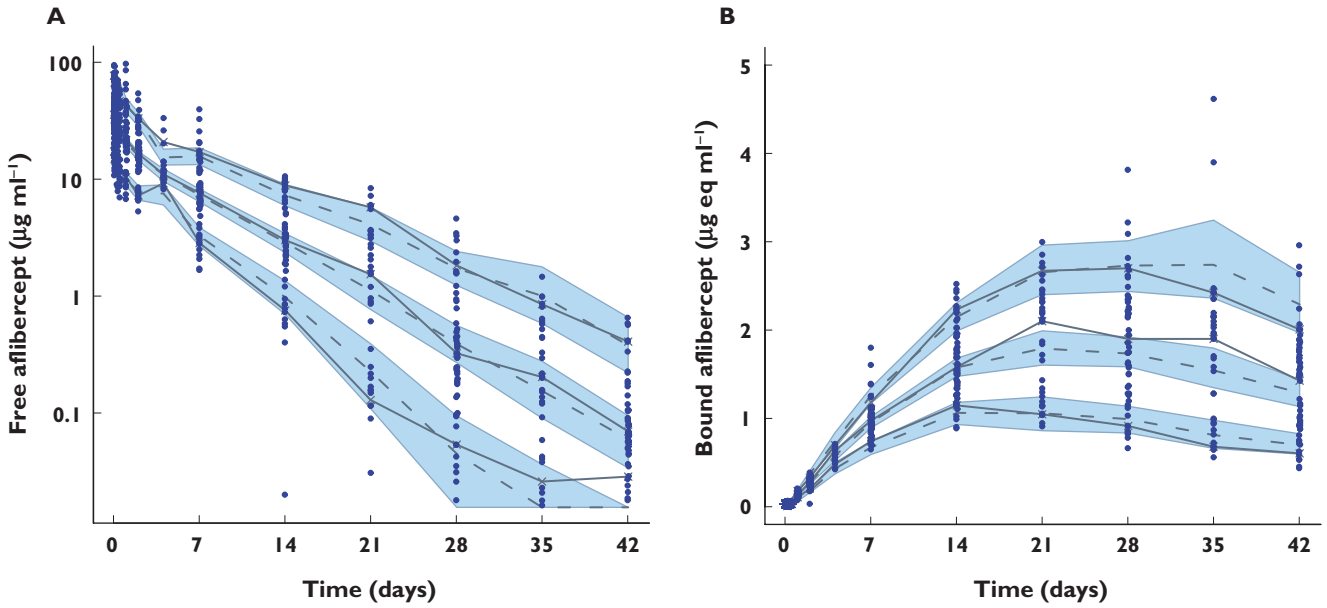

Figure 5

Visual predictive check (VPC) of free aflibercept in semi-logarithmic scale (A), and bound afibercept in linear scale (B) for the final model. Observed data are plotted using a solid circle (●) and censored data are plotted using a star (*). The shaded area and the dotted lines represent the 90% prediction interval and the predicted median of 10th, 50th and 90th percentiles of simulated data ($n = 500$). The solid lines represent the 10th, 50th and 90th percentiles of observed data

semi-logarithmic scale. The slight misfit for free aflibercept seen at the last time point may be a consequence of the number of concentrations near the LOQ, since the median and upper boundary appear to be very well predicted by the model. For bound aflibercept, the model slightly underpredicted median concentration from day 21 onwards but correctly predicted the variability. Thus, the model described reasonably well the observed concentrations of both free and bound aflibercept.

Discussion

In this study, we report the development of a mechanism-based model to characterize the population PK of aflibercept after a single i.v. infusion of a 2 to 4 mg kg^{-1} dose to 56 healthy subjects. Free and bound aflibercept plasma concentrations were used in the modelling.

We first modelled free aflibercept concentrations alone. Using standard compartmental PK models, we observed a decrease of clearance for higher concentrations. This was consistent with previous results from noncompartemental analyses, which demonstrated that the volume of distribution of free aflibercept was low and its clearance was dose-dependent. When dealing with saturable kinetics, the most common model to consider is MM elimination kinetics, which was retained as the final model for free aflibercept during model development. Although such a model has been successfully applied to describe nonlinear PK of free aflibercept, it does not represent well the underlying molecular events such as target binding, internalization and degradation of the drug. However, the modelling of free aflibercept helped us get general information about the model structure: two-compartment kinetics and dose-dependent clearance. More complex models combining linear and nonlinear elimination were also tested. They adequately fitted the data but were not retained as the final model of free aflibercept according to the statistical criteria.

The next step of modelling was then to add bound aflibercept data, which served as a marker of efficacy by representing the amount of VEGF bound to aflibercept. The mechanism of action of this drug suggested the use of TMDD model. Among several types, the MM approximation of the TMDD model developed by Gibiansky *et al*. [13] proved the most appropriate to reflect the kinetics of aflibercept in our study as free aflibercept concentrations were much higher than target concentrations and their binding to VEGF resulted in a fully saturated target. The relatively low concentration of free circulating VEGF was confirmed by the range of 19–47 pg ml^{-1} for plasma VEGF concentrations observed in healthy subjects in a meta-analysis [17]. In order to model simultaneously both free and bound drug, the MM equation of bound aflbercept was added into the system of differential equations. Free aflibercept is therefore eliminated through two pathways: non saturable elimination from the central compartment (k_{el}) and a specific and saturable binding to VEGF, followed by internalization (k_{int}) of bound aflibercept, which is its dominant elimination pathway. In addition, the formation

of bound aflibercept could occur predominantly in central or peripheral compartment. The final PK model was an approximate TMDD model involving two compartments for free aflibercept and one compartment for bound aflibercept, with MM type binding of free aflibercept to VEGF from the peripheral compartment.

The first-order dissociation rate constant (k_{off}) of the complex to give back free aflibercept was assumed to be negligible. Bound aflibercept might dominantly eliminate by internalization ($k_{int} >> k_{off}$). This assumption is reasonable and consistent with the study of Eppler *et al*. on the development of a TMDD model for recombinant human VEGF (rhVEGF) after i.v. administration in patients with coronary artery disease [18]. VEGF binding to its high affinity receptors was concluded as an essentially irreversible process *in vivo*. Aflibercept might have the same properties because this drug is produced from two high affinity receptors of aflibercept (VEGFR1 and 2).

Recently, a new derivation of MM approximation of TMDD, called the irreversible binding MM model has been proposed by Gibiansky *et al*. when the dissociation rate constant is negligible and the free target concentration is much smaller than the free drug concentration [19]. The developed model of aflibercept is therefore close to this new approximation of the TMDD model. The only difference is that an extra differential equation was added to describe the evolution of bound drug. The MM parameters in the final model represent the combinations of the TMDD model parameters: $V_{max} = k_{syn} \cdot V_R$ and $K_m = K_{IB} = k_{deg}/k_{on}$, where V_R is the volume of distribution of target and K_{IB}, k_{syn}, k_{deg} are the irreversible binding constant, target production rate and target degradation rate, respectively. Although these estimates are not sufficient for the complete description of the full TMDD model, they can provide useful information about the underlying kinetics of drug and target.

During the model development, the general TMDD model with k_{on} and k_{off} was also implemented, assuming that the total target concentration was constant. Free VEGF was then the difference between total VEGF and VEGF binding to aflibercept. This model showed that k_{on} and k_{off} could not be estimated separately with very small value of k_{off} and its poor precision. Removing k_{off} resulted in the model developed by Epper *et al*. [18], but we obtained unsatisfactory fits for bound aflibercept, either for central or peripheral binding to VEGF. A plateau phase after reaching the peak, instead of a decreasing phase was predicted for bound aflibercept and the predicted peak was lower.

Alternatively, we also evaluated the linear central or peripheral binding models with a first-order association rate constant (k_{on}) instead of V_{max} and K_m. These models did not describe the observed concentrations of bound aflibercept well, specifically the decreasing phase which illustrated the elimination of bound alibercept after reaching the peak was poorly approached. They were also found less appropriate by statistical criteria.

The nonlinear peripheral binding model was found to describe better the kinetics of drugs than the central binding one, which was consistent with the previous studies on the distribution of VEGF in the body [17]. Large quantities of VEGF were reported in the extravascular space of tumour and skeletal muscle [17], suggesting an important source of endogenous VEGF in the peripheral compartment and supporting our choice of final model. The plasma concentrations of bound aflibercept in the data were assumed to be the same as those in the peripheral compartment, with rapid transfer between extravascular and plasma space.

In the final model, the clearance of bound aflibercept was found to be 6.3 times lower than that of free aflibercept from the central compartment (0.14 l day^{-1} and 0.88 l day^{-1}, respectively). Both free and bound aflibercept were eliminated quite slowly. The typical central volume of distribution of free aflibercept was 4.94 l, indicating that free aflibercept has a low level of tissue diffusion and that it circulates mostly in the extravascular spaces. The volume of distribution of bound aflibercept was close to that of free aflibercept, which was observed in intermediate models and was fixed to the mean value of V_p in the final model due to the problem of identifiability. In the prior non-compartmental analysis of free aflibercept, the average clearance was 0.97 l day^{-1} and the steady-state volume of distribution was 5.98 l. These values were similar to those estimated by the modelling approach. Compared with a similar anti-angiogenic agent, bevacizumab, the central volume of distribution was close but the clearance of total aflibercept was nearly four times faster than that of total bevacizumab [20]. From MM parameters, the production rate of VEGF and the irreversible binding constant were calculated to be 0.99 mg day^{-1} and 2.91 μg ml^{-1} or 19909 pM, respectively. The irreversible binding constant was much larger than the *in vitro* binding affinity K_d observed for VEGF-A. Such a difference is due to the negligible value of k_{off} *in vivo* and it means that the target degradation rate (k_{deg}) is significantly faster than the dissociation rate (k_{off}).

The advantage of this study is the availability of drug concentration data with free and bound forms since they were separately assayed, which is not the case for many antibody products. Generally, only total drug, representing the sum of free and bound was assayed [20–22]. The pharmacokinetic analysis of total drug could not provide a good explanation of the mechanism of action of the drug, including the binding to the target; neither was it able to characterize well its pharmacokinetic profile. For example, a simple model of two-compartment infusion with first-order elimination was published for bevacizumab and squalamine, two anti-angiogenic agents dosed in total form [20, 21]. The availability of complex data for aflibercept helped us to characterize both the linear and non linear elimination pathways, as well as the complex internalization, and estimate the mechanistic parameters of the

TMDD system. This could not be achieved using a classical MM model of free drug alone. The concentrations of bound aflibercept could be considered as pharmacodynamic data information of this drug. Our model development was in agreement with the guidelines of modelling for drugs with TMDD properties as mentioned by Yan *et al*. [23]. To our knowledge, the model that we developed is the first mechanism-based population pharmacokinetic model for an anti-VEGF drug.

In conclusion, the present PK model for aflibercept characterizes well the underlying mechanism of disposition of aflibercept, where a saturable, high-affinity binding of aflibercept to its pharmacologic target (VEGF) is responsible for the observed nonlinear pharmacokinetic behaviour of the free drug. Although further studies will be needed to assess the influence of covariates because of the limited size of the present sample, this model helps to understand the properties of aflibercept better and provides a useful support for further studies in patients during the clinical development, in particular the determination of therapeutic doses using bound aflibercept concentrations as a marker of VEGF inhibition.

Competing Interests

Hoai-Thu Thai received a research grant from Sanofi-aventis to perform this research and is now doing a PhD funded by a research grant from Sanofi-aventis. Emmanuelle Comets acted as a consultant for Sanofi-aventis in 2009–10. France Mentré is the director of Inserm UMR 738 which receives a research grant from Sanofi-aventis and has been paid for running an education program at Sanofi-Aventis. Christine Veyrat-Follet and Gerard Sanderink are employees of Sanofi-aventis. Nicole Vivier and Catherine Dubruc are former employees of Sanofi-aventis.

The authors thank Global Metabolism and the Pharmacokinetics Department, Sanofi-aventis, Paris which supported Hoai-Thu Thai by a research grant during this work.

APPENDIX: Model development

General peripheral model of target-mediated drug disposition [10, 11]:

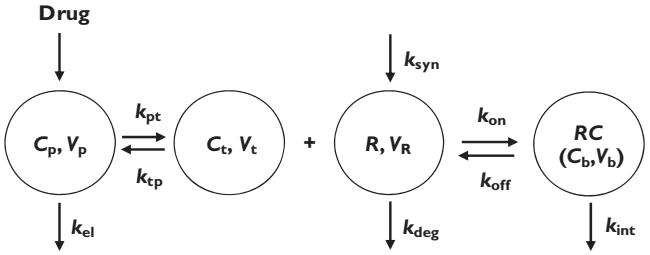

$$\frac{dC_p}{dt} = \text{Input} - (k_{el} + k_{pt}) \cdot C_p + k_{tp} \cdot \frac{C_t \cdot V_t}{V_p}$$
$$\frac{dC_t}{dt} = k_{pt} \cdot \frac{C_p \cdot V_p}{V_t} - k_{tp} \cdot C_t - \frac{k_{on} \cdot C_t \cdot R \cdot V_R}{V_t} + k_{off} \cdot \frac{C_b \cdot V_b}{V_t}$$
$$\frac{dC_b}{dt} = \frac{k_{on} \cdot C_t \cdot R \cdot V_R}{V_b} - k_{int} \cdot C_b - k_{off} \cdot C_b$$
$$\frac{dR}{dt} = k_{syn} - k_{deg} \cdot R - k_{on} \cdot C_t \cdot R + k_{off} \cdot \frac{C_b \cdot V_b}{V_R} \quad \text{(A1)}$$

where C_p, C_t, C_b, R are the concentrations of free drug in the central and peripheral compartment, complex (bound drug) and target, V_p, V_t are the volume of distribution of free drug in the central and peripheral compartment and V_R, V_b are the volume of distribution of target and bound drug in the peripheral compartment. k_{el} is the elimination rate of free drug from central compartment, k_{on}, k_{off} are the association and dissociation rate constants, k_{int} is the internalization rate constant of the complex and k_{syn}, k_{deg} are the target production and degradation rates.

To write this general model, we did not assume that the drug, the target and the bound drug have the same volume of distribution, and we assumed that the amount of bound drug created during a unit of time, produced in the compartment of distribution of the target, is $k_{on} \cdot R.C_t \cdot V_R$ [10, 11].

When the free drug concentrations are much higher than target concentrations ($C >> R$) and their binding results in a fully saturated target, the full TMDD can be replaced by the MM approximations of the TMDD model following the suggestions of Gibiansky *et al*. [13, 19]. We explain these approximations for peripheral TMDD models.

Approximation 1

The first MM approximation of TMDD model was proposed in case of reversible binding, based on the assumptions that the drug–target complex is in a quasi-steady-state or the derivative of the complex concentration, dC_b/dt, is zero [13]. V_R and V_b were assumed to be equal to V_t.

$$k_{on} \cdot C_t \cdot R - (k_{int} + k_{off}) \cdot C_b = 0 \quad \text{(A2)}$$

$$\frac{C_t \cdot R}{C_b} = \frac{k_{int} + k_{off}}{k_{on}} = K_{ss} \quad \text{(A3)}$$

$$C_b = \frac{R_{tot} \cdot C_t}{K_{ss} + C_t} \quad \text{(A4)}$$

where R_{tot} is the total concentration of target ($R_{tot} = R + C_b$).

We can rearrange the equation for dC_t/dt, by expressing C_b as a function of C_t and using the expression of K_{ss}, yielding the following equation:

$$\frac{dC_t}{dt} = k_{pt} \cdot \frac{C_p \cdot V_p}{V_t} - k_{tp} \cdot C_t - \frac{k_{int} \cdot R_{tot} \cdot C_t}{K_{ss} + C_t} \quad \text{(A5)}$$

This new equation dC_t/dt therefore includes a MM type elimination with

$$V_{max} = R_{tot} \cdot k_{int}; K_m = K_{ss} = (k_{int} + k_{off})/k_{on} \quad \text{(A6)}$$

If, in addition, the total target concentration R_{tot} can be considered constant, V_{max} is a constant parameter of the system. The TMDD equation system then results in the two following equations:

$$\frac{dC_p}{dt} = \text{Input} - (k_{el} + k_{pt}) \cdot C_p + k_{tp} \cdot \frac{C_t \cdot V_t}{V_p}$$
$$\frac{dC_t}{dt} = k_{pt} \cdot \frac{C_p \cdot V_p}{V_t} - k_{tp} \cdot C_t - \frac{V_{max} \cdot C_t}{K_m + C_t} \quad \text{(A7)}$$

Approximation 2

When the binding is irreversible, the dissociation binding rate constant $k_{off} = 0$ then the TMDD equations simplify:

$$\frac{dC_p}{dt} = \text{Input} - (k_{el} + k_{pt}) \cdot C_p + k_{tp} \cdot \frac{C_t \cdot V_t}{V_p}$$
$$\frac{dC_t}{dt} = k_{pt} \cdot \frac{C_p \cdot V_p}{V_t} - k_{tp} \cdot C_t - \frac{k_{on} \cdot C_t \cdot R \cdot V_R}{V_t}$$
$$\frac{dC_b}{dt} = \frac{k_{on} \cdot C_t \cdot R \cdot V_R}{V_b} - k_{int} \cdot C_b$$
$$\frac{dR}{dt} = k_{syn} - k_{deg} \cdot R - k_{on} \cdot C_t \cdot R \quad \text{(A8)}$$

The second MM approximation of the TMDD models was proposed in the case of irreversible binding. It is based on the assumption that the target is in a quasi steady-state so that the derivative of target concentration, *dR/dt*, is zero [19].

$$k_{syn} - k_{deg} \cdot R - k_{on} \cdot C_t \cdot R = 0 \quad \text{(A9)}$$

$$R = \frac{k_{syn}}{k_{deg} + k_{on} \cdot C_t} = \frac{R_0 \cdot K_{IB}}{K_{IB} + C_t} \quad \text{(A10)}$$

where K_{IB} is the irreversible binding constant ($K_{IB} = k_{deg}/k_{on}$) and R_0 is the target concentration at baseline ($R_0 = k_{syn}/k_{deg}$), which can be obtained assuming steady-state in the differential equation for R in the absence of drug.

Using this expression for R and noticing that $R_0 \cdot K_{IB} \cdot k_{on} = k_{syn}$, we can simplify the equation for dC_t/dt to:

$$\frac{dC_t}{dt} = k_{pt} \cdot \frac{C_p \cdot V_p}{V_t} - k_{tp} \cdot C_t - \frac{1}{V_t} \cdot \frac{k_{syn} \cdot V_R \cdot C_t}{K_{IB} + C_t} \quad \text{(A11)}$$

Also, generally, only free drug is measured, so that in their model, Gibiansky *et al*. did not take into account the evolution of the complex (dC_b/dt) [19]. The TMDD equation system therefore includes only two equations:

$$\frac{dC_p}{dt} = \text{Input} - (k_{el} + k_{pt}) \cdot C_p + k_{tp} \cdot \frac{C_t \cdot V_t}{V_p}$$
$$\frac{dC_t}{dt} = k_{pt} \cdot \frac{C_p \cdot V_p}{V_t} - k_{tp} \cdot C_t - \frac{1}{V_t} \cdot \frac{k_{syn} \cdot V_R \cdot C_t}{K_{IB} + C_t} \quad \text{(A12)}$$

Application to our study

In our case, the free aflibercept concentrations were much higher than the target concentrations. We also considered the evolution of bound aflibercept since the concentrations of bound aflibercept were available and could not be considered negligible in the system. In addition, the dissociation rate constant was found to be very small during model development so that irreversible binding and the negligible change in target concentrations (*dR/dt*) could be assumed, which is similar to the assumptions of the second MM approximation described above. Thus, our differential equation system is (A12) to which we add the equation for dC_b/dt from (A8) where $k_{off} = 0$.

Substituting the expression for $R = \frac{R_0 \cdot K_{IB}}{K_{IB} + C_t}$ derived from the second assumption of TMDD model, we find the following expression:

$$\frac{dC_p}{dt} = \text{Input} - (k_{el} + k_{pt}) \cdot C_p + k_{tp} \cdot \frac{C_t \cdot V_t}{V_p}$$
$$\frac{dC_t}{dt} = k_{pt} \cdot \frac{C_p \cdot V_p}{V_t} - k_{tp} \cdot C_t - \frac{1}{V_t} \cdot \frac{k_{syn} \cdot V_R \cdot C_t}{K_{IB} + C_t}$$
$$\frac{dC_b}{dt} = \frac{1}{V_b} \frac{k_{syn} \cdot V_R \cdot C_t}{K_{IB} + C_t} - k_{int} \cdot C_b \quad \text{(A13)}$$

Again, we notice a MM elimination for equation dC_t/dt, which enters the equation of dC_b/dt as a saturable input.

This equation system can be written with MM parameters, which represents our final model:

$$\frac{dC_p}{dt} = \text{Input} - (k_{el} + k_{pt}) \cdot C_p + k_{tp} \cdot \frac{C_t \cdot V_t}{V_p}$$
$$\frac{dC_t}{dt} = k_{pt} \cdot \frac{C_p \cdot V_p}{V_t} - k_{tp} \cdot C_t - \frac{1}{V_t} \cdot \frac{V_{max} \cdot C_t}{K_m + C_t}$$
$$\frac{dC_b}{dt} = \frac{1}{V_b} \cdot \frac{V_{max} \cdot C_t}{K_m + C_t} - k_{int} \cdot C_b \quad \text{(A14)}$$

where $V_{max} = k_{syn}.V_R = A_{syn}$ and $K_m = K_{IB}$.

For parameter estimation, the micro constants (k_{el}, k_{pt}, k_{tp}) can be replaced by the macro constants: $Q = k_{tp} \cdot V_t = k_{pt} \cdot V_p$ and $CL = k_{el} \cdot V_p$, where CL is the clearance of free drug from the central compartment and Q is the intercompartment clearance of free drug.

REFERENCES

1 Baka S, Clamp AR, Jayson GC. A review of the latest clinical compounds to inhibit VEGF in pathological angiogenesis. Expert Opin Ther Targets 2006; 10: 867–76.

2 Folkman J, Merler E, Abernathy C, Williams G. Isolation of a tumor factor responsible for angiogenesis. J Exp Med 1971; 133: 275–88.

3 Holash J, Davis S, Papadopoulos N, Croll SD, Ho L, Russell M, Boland P, Leidich R, Hylton D, Burova E, Ioffe E, Huang T, Radziejewski C, Bailey K, Fandl JP, Daly T, Wiegand SJ, Yancopoulos GD, Rudge JS. VEGF-Trap: a VEGF blocker with potent antitumor effects. Proc Natl Acad Sci U S A 2002; 99: 11393–8.

4 Moreira IS, Fernandes PA, Ramos MJ. Vascular endothelial growth factor (VEGF) inhibition – a critical review. Anticancer Agents Med Chem 2007; 7: 223–45.

5 Salven P, Manpaa H, Orpana A, Alitalo K, Joensuu H. Serum vascular endothelial growth factor is often elevated in disseminated cancer. Clin Cancer Res 1997; 3: 647–51.

6 Ferrara N. Vascular endothelial growth factor: basic science and clinical progress. Endocrinol Rev 2004; 25: 581–611.

7 Chu QS. Aflibercept (AVE0005): an alternative strategy for inhibiting tumour angiogenesis by vascular endothelial growth factors. Expert Opin Biol Ther 2009; 9: 263–71.

8 Lockhart AC, Rothenberg ML, Dupont J, Cooper W, Chevalier P, Sternas L, Buzenet G, Koehler E, Sosman JA, Schwartz LH, Gultekin DH, Koutcher JA, Donnelly EF, Andal R, Dancy I, Spriggs DR, Tew WP. Phase I study of intravenous vascular endothelial growth factor Trap, aflibercept, in patients with advanced solid tumors. J Clin Oncol 2009; 28: 207–14.

9 Sternberg CN. Systemic chemotherapy and new experimental approaches in the treatment of metastatic prostate cancer. Ann Oncol 2008; 19 (Suppl. 7): vii91–5.

10 Mager DE, Jusko WJ. General pharmacokinetic model for drugs exhibiting target-mediated drug disposition. J Pharmacokinet Pharmacodyn 2001; 28: 507–32.

11 Mager DE. Target-mediated drug disposition and dynamics. Biochem Pharmacol 2006; 72: 1–10.

12 Mager DE, Krzyzanski W. Quasi-equilibrium pharmacokinetic model for drugs exhibiting target-mediated drug disposition. Pharm Res 2005; 22: 1589–96.

13 Gibiansky L, Gibiansky E, Kakkar T, Ma P. Approximations of the target-mediated drug disposition model and identifiability of model parameters. J Pharmacokinet Pharmacodyn 2008; 35: 573–91.

14 Samson A, Lavielle M, Mentre F. Extension of the SAEM algorithm to left-censored data in nonlinear mixed-effects model: application to HIV dynamics model. Comput Stat Data Anal 2006; 51: 1562–74.

15 Bertrand J, Comets E, Mentre F. Comparison of model-based tests and selection strategies to detect genetic polymorphisms influencing pharmacokinetic parameters. J Biopharm Stat 2008; 18: 1084–102.

16 Brendel K, Comets E, Laffont C, Laveille C, Mentre F. Metrics for external model evaluation with an application to the population pharmacokinetics of gliclazide. Pharm Res 2006; 23: 2036–49.

17 Kut C, Mac Gabhann F, Popel AS. Where is VEGF in the body? A meta-analysis of VEGF distribution in cancer. Br J Cancer 2007; 97: 978–85.

18 Eppler SM, Combs DL, Henry TD, Lopez JJ, Ellis SG, Yi JH, Annex BH, McCluskey ER, Zioncheck TF. A target-mediated model to describe the pharmacokinetics and hemodynamic effects of recombinant human vascular endothelial growth factor in humans. Clin Pharmacol Ther 2002; 72: 20–32.

19 Gibiansky L, Gibiansky E. Target-mediated drug disposition: new derivation of the Michaelis-Menten model, and why it is often sufficient for description of drugs with TMDD. 2010. PAGE 19; Abstr 1728. Available at http://www.page-meeting.org/?abstract=1728 (last accessed 14 June 2011).

20 Lu JF, Bruno R, Eppler S, Novotny W, Lum B, Gaudreault J. Clinical pharmacokinetics of bevacizumab in patients with solid tumors. Cancer Chemother Pharmacol 2008; 62: 779–86.

21 Bhargava P, Marshall JL, Dahut W, Rizvi N, Trocky N, Williams JI, Hait H, Song S, Holroyd KJ, Hawkins MJ. A phase I pharmacokinetic study of squalamine, a novel antiangiogenic agent, in patients with advanced cancers. Clin Cancer Res 2001; 7: 3912–9.

22 Hayashi N, Tsukamoto Y, Sallas WM, Lowe PJ. A mechanism-based binding model for the population pharmacokinetics and pharmacodynamics of omalizumab. Br J Clin Pharmacol 2007; 63: 548–61.

23 Yan X, Mager DE, Krzyzanski W. Selection between Michaelis-Menten and target-mediated drug disposition pharmacokinetic models. J Pharmacokinet Pharmacodyn 2010; 37: 25–47.